Research article

Facilitation stabilizes moisture-controlled alpine juniper shrublines in the central Tibetan Plateau

Yafeng Wang[a], Eryuan Liang[a, b*], Aaron M. Ellison[c], Xiaoming Lu[a, d] and J. Julio Camarero[e]

[a]Key Laboratory of Alpine Ecology and Biodiversity, Key Laboratory of Tibetan Environment Changes and Land Surface Processes, Institute of Tibetan Plateau Research, Chinese Academy of Sciences, Beijing 100085, China

[b]CAS Center for Excellence in Tibetan Plateau Earth Sciences, Beijing 100101, China

[c]Harvard Forest, 324 North Main Street, Petersham, MA 01366, USA

[d]University of Chinese Academy of Science, Beijing 100000, China

[e]Instituto Pirenaico de Ecología (IPE-CSIC), Avda. Montañana, 1005, 50080 Zaragoza, Spain

Corresponding author: Dr. Eryuan Liang, Liangey@itpcas.ac.cn

ABSTRACT

The Tibetan Plateau hosts one of the world's highest undisturbed alpine juniper shrublines. However, little is known about the dynamics of these shrublines in response to climate warming and shrub-to-shrub interactions. Since growth of shrubline junipers is limited more by moisture availability than by low temperatures, we tested if upslope advancement of alpine juniper shrublines was constrained by warmer temperatures and related recent droughts. We also evaluated whether facilitation among neighboring shrubs, as inferred from spatial analyses, influenced shrubline dynamics. Three rectangular plots crossing the *Juniperus pingii* var. *wilsonii* shrubline were sampled at elevations from 4810 to 4917 m a.s.l. near the Nam Co Lake, central Tibetan Plateau. Location of each stem and its diameter at the root collar and age were measured. We reconstructed the spatial and temporal shrubline dynamics during the past 350 years using standard dendrochronological methods. Independent, long-term summer temperature reconstructions also were associated with shrub recruitment. Point-pattern analyses were used to characterize spatial patterns of different size classes of shrubs. The three shrublines showed little long-term changes despite ongoing warming; no upward shift has occurred in the past 100 years. Recruitment was negatively associated with summer temperatures and drought occurrence since the 1920s. Spatial patterns were characterized by clustering at local scales and attraction between the different size classes, suggesting facilitation. We conclude that moisture availability limits the recruitment and elevational advance of junipers in this area of the Tibetan Plateau. Dynamics of alpine shrublines are more

contingent on positive interactions and local environmental factors than on regional climatic variability.

Keywords:

Dendroecology; alpine shrubline; climatic warming; conspecific facilitation; drought; Tibetan Plateau.

1. Introduction

A growing body of evidence shows that global climatic warming has been altering the composition, structure, and distribution of ecosystems worldwide (IPCC, 2014). Among these structural changes, the northern or upward expansion of shrublines—the highest latitude or uppermost altitude at which shrubs occur—into arctic tundra or alpine grasslands is often regarded as fingerprint of global climate warming (Sturm et al., 2001; Post et al., 2009). However, little is known about the range shift of alpine shrublines in mid-latitude mountains subjected to predictable seasonal changes in precipitation and moisture availability, even though alpine shrublands are a major community in these treeless regions (Körner, 2003).

Climatic warming is expected to lead to shifts of latitudinal or altitudinal treelines and shrublines (Kullman, 2002; Myers-Smith et al., 2011; Hofgaard et al., 2013) because minimum air and soil temperatures set the frame for the processes at the leading edge of woody plant communities (Fang et al., 2009; Lv and Zhang, 2011; Liu and Yin, 2013). However, in areas subjected to seasonal water deficits, positive effects of warming on local treelines or shrublines could be canceled out without concurrent increases in precipitation that would alleviate heat-induced moisture stress (Daniels and Veblen, 2004; Wahren et al., 2005). For example, where plant growth at alpine treeline or shrubline is limited by moisture availability during the early growing season (Liang et al., 2012, 2014) or the previous winter (Pellizzari et al., 2014), the treelines or shrublines could be at risk of retreat if lack of water leads to growth decline, constrains recruitment, or increases mortality rates.

Local site conditions (e.g., disturbance, topography, biotic interactions) also buffer, nullify, or alter climatic impacts on treelines and shrublines (Callaway et al., 2002; Kikvidze et al., 2005; Case and Duncan, 2014), resulting in heterogeneous and locally contingent responses of nearby ecotones to shared climatic forcing (Harsch et al., 2009). Among those local factors, plant-plant interactions increasingly are thought to be major drivers of treeline and shrubline dynamics (Batllori et al., 2009; Grau et al., 2012). However, surprisingly little information is available about whether such interactions play a role in mediating alpine shrubline dynamics as the climate warms (Dullinger et al., 2011).

One of the world's highest natural alpine shrublines occurs on the Tibetan Plateau (Wu, 1983; Huang and Zhang, 2011). In these cold, dry, and treeless regions, shrublands are the primary locus of nutrient cycling, water flow regulation, carbon sequestration, and biodiversity (Huang and Zhang, 2011). However, little is known about the impacts of climatic warming on the structure and distribution of alpine shrublines. *Juniperus pingii* var. *wilsonii* (Rehder) Silba is a widespread alpine shrub forming the upper shrubline across the central Tibetan Plateau at elevations over 4900 m. The extremely harsh climatic conditions experienced at the upper limit of shrubs lead to a relatively narrow ecotone of less than 100-m between the shrubline and other alpine vegetation devoid of taller shrub species.

Here we assess how regional climatic conditions and local-scale biotic interactions (cf. Callaway et al., 2002) affect dynamics at three high-elevation *J. pingii* var. *wilsonii* shrublines. Specifically, we: (1) reconstructed the age structure of individual

shrubs; (2) revealed alpine shrubline dynamics on multi-centennial time scales; and (3) inferred underlying processes of shrubline dynamics from spatial point-pattern analyses of different size classes of shrubs. Our earlier research had shown that the radial growth of *J. pingii* var. *wilsonii* is limited by scarce precipitation rather than by low temperature (Liang et al., 2012). Thus, we hypothesized that on the three shrublines we studied that the upslope advancement of the shrubline would be constrained by recent warming-related droughts. Further, because patchy patterns in alpine shrublands across harsh environments can reflect intraspecific facilitation (Choler et al., 2001; Armas and Pugnaire, 2005), we also hypothesized that positive conspecific interactions would be reflected in clustered spatial patterns of individual junipers.

2. Materials and methods

2.1 Study area and climate

The study area is located near the Nam Co Lake (30° 30’ - 30° 55’ N; 90° 16’- 91° 03’ E; 4725 m a.s.l.) on the northern flank of the Gangdise-Nyainqintanglha Mountains (Zhu et al., 2010). Climatically, this area is in the transition zone between semi-arid and sub-humid conditions. Between 2006 and 2008, the annual average temperature at 4730 m a.s.l. on the southeastern shore of the lake (AWS in Fig. 1a), was 0.4°C. January (−8.4 °C) and July (9.5 °C) were the coldest and warmest months, respectively (Zhang et al. 2011). The mean annual precipitation was 415 mm, ≈85% of which fell between July and October (Zhang et al., 2011). However, the climate

was dry in May and June, when mean monthly precipitation was, respectively, < 15 and 35 mm, and mean monthly evaporation was > 130 and 160 mm (Zhang et al., 2011). Average daily wind speed was low (3.6 $m.s^{-1}$; see also Zhang et al. 2011) and southeasterly dry winds dominated during the growing season. At the meteorological station of Baingoin (4700 m a.s.l.), about 100 km north-west of the Nam Co Lake, monthly mean temperature, monthly total precipitation, and evaporation from 1957 to 2013 illustrated the dry and cold climates in central Tibet (Fig. 2). Temperature reconstructions from different regions on the Tibetan Plateau and based on tree-ring or ice-core proxies identified a warming trend in the area over the past 400 years (Bräuning and Mantwill, 2004; Liu et al., 2005; Liu et al., 2009; Yang et al., 2009) but no significant change in reconstructed annual precipitation over the same interval (Yao et al., 2008).

2.2 Study species

J. pingii var. *wilsonii* (henceforth "juniper") is the most widely distributed shrub species on the Tibetan Plateau (Huang and Zhang, 2011). In the central Tibetan Plateau and around the Nam Co Lake, junipers grow as prostrate, multi-stemmed shrubs in cushion-forming patches of multiple individuals on south-facing slopes; isolated individuals are rarely observed. Their maximum crown diameter is ≤ 3 m, they rarely exceed 1.5 m in height (Chen and Yang, 2011), and the stem diameter at the root collar is normally < 20 cm.

On the central Tibetan Plateau, junipers grow along an altitudinal gradient from

141 4,740 m to above 4,900 m a.s.l. The most abundant herb species located above the
142 studied juniper shrubline are: *Rhodiola fastigiata* (Hook. f. et Thoms.) S. H. Fu,
143 *Corydalis thyrsiflora* Prain, *Oxytropis glacialis* Benth. ex Bunge, *Astragalus arnoldii*
144 Hemsl., *Euphorbia stracheyi* Boiss., *Stellera chamaejasme* Linn., *Heracleum*
145 *millefolium* Diels., *Androsace tapete* Maxim., *Phlomis younghusbandii* Mukerjee,
146 *Oreosolen wattii* Hook. f, *Morina kokonorica* Hao and *Carex oxyleuca* V. Krecz.
147 Human disturbance at the upper elevational limits of juniper usually is negligible
148 because they are remote and lack of edible grass for grazing yaks; cover of edible
149 grass species such as *Stipa purpurea* Griseb. accounts for < 5% cover at the shrubline
150 ecotone. We did not observe any sign of grazing by yaks while we were doing
151 fieldwork in 2013 or 2014, nor did we detect other evidence of human disturbances,
152 such as remains of charcoal, fire scars, browsing damage, or stumps in the study sites.
153 Annual growth rate of juniper is very slow; ring widths average 0.29 ± 0.15
154 mm/yr. Series-sectioning, i.e., comparison of ring-growth series from several sections
155 taken along one shoot of the same individual (methodological details in Kolishchuk,
156 1990; Wilmking et al., 2012), confirmed that the cambium along juniper stems
157 remains active. As a result, we were unlikely to miss outer rings in basal stem sections
158 (Liang et al., 2012). Despite juniper's slow growth, annual ring-width series from
159 different individuals can be cross-dated (Liang et al., 2012; see also the robust
160 cross-dating for other similar shrub species reviewed by Myers-Smith et al., 2015).
161 Radial growth of junipers is limited primarily by low moisture availability in
162 May-June during the year of ring formation (Liang et al., 2012).

163

164 *2.3 Field sampling*

165 In July and August, 2013, we sampled three rectangular plots (30 m × 120 m)
166 located near the north-eastern shore of Nam Co Lake (Fig. 1b). Two plots (SE1, SE2)
167 faced southeast (plot SE1: 30.89° N, 90.86° E, 4866 m a.s.l., slope 18°; plot SE2:
168 30.91° N, 90.80° E, 4917 m, slope 13°), whereas the third (SW1) faced southwest
169 (plot SW1: 30.89° N, 90.87° E, 4810 m, slope 20°). Each rectangular plot was located
170 in a topographically uniform part of the shrubline ecotone. The long side of the plot
171 paralleled the maximum slope and extended above the shrubline (see also Camarero
172 and Gutiérrez, 2004). The relative origin for each plot was situated in its lower left
173 corner. Elevations of lower and upper edges of the plots were measured using a GPS
174 calibrated with a barometric altimeter. Locations (as x, y coordinates ± 0.1 m) of the
175 main stem of each individual shrub within each plot were recorded. Two additional
176 variables for each shrub also were recorded: its maximum height and the diameter at
177 the root collar of the thickest stem of each individual. An electronic caliper was used
178 to measure the stem diameter (± 0.01 mm) and tapes were employed to measure shrub
179 height (± 10 cm). We did not find any dead shrubs within any of the plots.

180 The age structure of shrubs within the three study plots was obtained using
181 dendrochronological methods (Camarero and Gutiérrez, 2004), as have been used to
182 document shrubline changes in recent years (Myers-Smith et al., 2015). An increasing
183 number of treeline studies have explored recruitment dynamics using static age
184 structures, which reflect the balance between survival and mortality rate (Camarero

and Gutiérrez, 2004; Liang et al., 2011). Due to the dense wood and small size of shrub stems, collecting discs, not increment cores, are used frequently in the Tibetan Plateau and the Arctic to measure their growth rings of shrubs and relate shrub growth to climate (see reviews in Myers-Smith et al., 2015). In fact, we broke several increment borers during field investigation. However, because sampling stem discs destroy the stem, we could not collect discs from every juniper in the plot. Rather, we first randomly collected 22, 36, and 33 discs from individual junipers just outside of plots SE1, SW1 and SE1, respectively. These samples were visually cross-dated using characteristic rings, yielding inter-correlations for samples from sites SE1, SW1, and SW2 of 0.62, 0.58, and 0.61, respectively.

Second, we established relationships between age and root-collar of junipers from 80 randomly-sampled individuals in plot SE2. Wood discs were cut from the thickest stem of each individual shrub, as closely as possible to the root collar; disc diameters ranged from 2.0 to 18.3 cm, and ages ranged from 39 to 361 years. Based on linear relationships between stem diameter at the root collar and juniper age (Fig. 3a), ages of all junipers measured in all three plots were estimated to the nearest decade.

2.4 Characterizing shrubline dynamics

We observed that mature shrubs < 1 m tall may be > 250 years old (Liang et al., 2012). Thus, it made little sense to define the location of the shrubline by shrub height because height growth is very slow and unrelated to age (Fig. 3). Rather, changes in

207 the upper elevation of the shrubline in the three study plots were reconstructed for the
208 past 350 years (i.e., 1664 -2013) in 50-year intervals based on mapping junipers and
209 estimating their establishment dates to the nearest decade (from the relationship
210 shown in Fig. 3a). Establishment dates were then related to reconstructed summer
211 temperatures on the Tibetan Plateau (Thompson et al., 2006).
212
213 *2.5 Point pattern analyses*
214 Spatial statistics are efficient tools to analyze vegetation dynamics using space as
215 a surrogate to test hypotheses and to infer underlying (and usually unmeasured)
216 processes (Fortin and Dale, 2005; McIntire and Fajardo, 2009; Wang et al., 2010).
217 Point-pattern analyses were used to characterize spatial patterns of junipers growing
218 in the three study plots. We used the $O(r)$ statistic (Wiegand and Moloney, 2004;
219 Wang et al., 2010) to compare observed spatial patterns with those expected under a
220 null model of complete spatial randomness (CSR). Aggregated or hyperdispersed
221 (regular) distributions have values of $O(r)$ higher and lower than λ, respectively,
222 where λ is the value obtained for $O(r)$ for a CSR pattern of the same sample size. Note
223 that the $O(r)$ statistic is a scale-dependent probability density function related to a
224 neighbourhood density (Wiegand and Moloney, 2004). Considering that both the
225 mean radius of shrub patches and the distances between the nearest patches were no
226 more than 5 m, respectively, we calculated $O(r)$ at a spatial resolution = 1 m and for
227 spatial scales ranging from 1 to 10 m, which should identify relevant small-scale
228 patterns in the study plots. Last, because the plots are environmentally heterogeneous

(in, e.g., soil conditions and microtopography), we used the inhomogeneous version of the $O(r)$ statistic for all point-pattern analyses. The Programita software was used to perform all point pattern analyses (Wiegand and Moloney, 2004, 2014).

2.5.1 Univariate point pattern analyses

We used the univariate $O_{11}(r)$ statistic to examine spatial patterns of three different size classes: size 1 (stem diameter at the root collar ≤ 3 cm); size 2 (3 < stem diameter ≤ 8 cm); and size 3 (stem diameter > 8 cm). These three size classes correspond to different age classes, because shrub size was found to be related to shrub age (Fig. 3a). Specifically, size classes 1, 2, and 3 corresponded to the following age classes: age ≤ 80 yrs, 80 yrs < age ≤ 150 years, and age > 150 years, respectively. Such classification agreed well with the distribution of shrub ages at the three study plots (Fig. 3b). We used a heterogeneous Poisson process as the null model to simulate CSR. Edge correction was used to ensure that the number of points in an incomplete circle was divided by the proportion of the area of the circle that lay within the study plot (Wiegand and Moloney, 2004, 2014). Finally, if the calculated $O_{11}(r)$ statistic was above or below the upper or lower 99% simulation envelopes based on 999 Monte Carlo simulations of the original data then the pattern was considered to be significantly aggregated or hyperdispersed (regular), respectively, at the analyzed spatial scale.

2.5.2 Bivariate point pattern analyses

We used the $O_{12}(r)$ statistic to study spatial associations between pairs of the three different size classes of shrubs. We assumed that larger shrub individuals (size 3 in this study) could influence smaller individuals (size 1 and 2), but not *vice versa*. Hence, we used an antecedent condition as the null model, which only randomized the locations of small individuals (sizes 1 or 2), while keeping fixed the locations of larger adults (size 3) or mid-size juveniles (size 2), respectively (Wiegand and Moloney, 2004, 2014). In this case, the statistic $O_{12}(r) = \lambda_2 g_{12}(r)$, for which $g_{12}(r)$ is the bivariate mark-correlation function, gives the expected number of points of pattern 2 (seedlings or mid-size juveniles) located at distance r from any point of pattern 1 (mid-size juveniles or adults). $O_{12}(r) = \lambda_2$ corresponds to independent patterns, whereas $O_{12}(r) < \lambda_2$ or $O_{12}(r) > \lambda_2$ corresponds to repulsion (negative association) and attraction (positive association), respectively (Wiegand and Moloney, 2004, 2014). If the $O_{12}(r)$ statistic was above or below the 99% upper or lower simulation envelopes, the pattern was considered to show significant positive or negative associations at those spatial scales, respectively.

3. Results

3.1 Size structure of junipers

Stem diameter classes were right-skewed and unimodal in all plots (Fig. 4). The maximum stem diameters at the root collar were 17.2, 20.2, and 25.5 cm in plots SE1, SW1, and SE2, respectively. Most junipers were < 80 cm tall, but the maximum height of individuals within the three plots ranged from 113 to 150 cm (Fig. 3c, d, e).

3.2 Climate and juniper establishment

The oldest junipers in plots SE1, SW1, and SE2, respectively, were estimated to be 351, 409, and 512 years in (Fig. 3b), but there were only one or two individuals older than 350 years in any of the plots. Reconstructed recruitment in each plot appeared to be common before 1950, but rare thereafter (Fig. 5). The relationship between reconstructed recruitment and reconstructed climate also differed before the 1920s, when recruitment and summer temperature were positively and significantly correlated (SE1, $r = 0.59$; SW1, $r = 0.58$; SE2, $r = 0.65$; in all cases $n = 33$ and $P < 0.001$), and after the 1920s, when they were negatively, but not significantly, correlated (SE1, $r = -0.36$; SW1, $r = -0.40$; SE2, $r = -0.39$; in all cases $n = 8$ and, $P > 0.05$).

3.3 Shrubline dynamics

Overall, the juniper shrublines in plots SE1, SW1, and SE2 have shifted upwards by 8, 4 and 9 m, respectively, in the past 350 years, but such summary values obscure much of the variability. In plot SE1 (Fig. 6a), the juniper shrubline increased 6 m in elevation during the 1714−1763 period relative to the previous 50 years. It then remained unchanged from 1764 to 1863, but shifted upward again by 1 m between 1864 and 1913 and by another 1 m between 1914 and 1963. In the last 50-year period, no change in shrubline elevation was observed in the data. In plot SW1 (Fig. 6b), the juniper shrubline increased in elevation by 2.0 m (1714−1763), was unchanged

295 (1764−1813), advanced again by 2 m (1814−1863), and then remained unchanged
296 thereafter. Finally, in plot SE2 (Fig. 6c), the juniper shrubline increased in elevation
297 by 4.0 m (1714-1763), ascended another 5.0 m (1764−1813), and then stopped
298 advancing.
299
300 *3.4 Spatial patterns of shrub size classes*
301 Considering all size-classes together, junipers in all sampled plots were
302 significantly aggregated at spatial scales of 1−10 m (in plots SE1 and SE2) or 1−7 m
303 (plot SW1). Among the three size classes, aggregated distributions in plot SE1 were
304 detected at spatial scales of 1−10 m (size-classes 1 and 2) or 1−3 m (size-class 3) (Fig.
305 7a). In this same plot, the three analyzed pairings among the size classes (size-class 1
306 *vs*. size-class 2, size-class 1 *vs*. size-class 3, and size-class 2 *vs*. size-class 3) were
307 positively associated at spatial scales from 1 to 6 m. In plot SW1, size-classes 1 and 2
308 were significantly aggregated from 1 to 6 m, but size-class 3 was CSR (Fig. 7b).
309 Bivariate analysis revealed that all size classes were positively associated from 1 to 3
310 m in plot SW1. In plot SE2, all three size classes were significantly aggregated at
311 spatial scales of 1−8 m (size-class 1), 1−3 m (size-class 2) and 1−2 m (size-class 3)
312 (Fig. 7c). In contrast to the other two plots, however, negative spatial associations
313 were found for SE3 between size-classes 1 and 3 at 1−7 m, whereas other pairs
314 (size-class 1 *vs*. size-class 2, size-class 2 *vs*. size-class 3) were significantly positively
315 associated at spatial scales from 1 to 10 m. Overall, spatial associations were stronger
316 between the larger size classes (size 2 *vs*. size 3) than between the smallest and bigger

317 classes (size 1 *vs*. size 2 or size 1 *vs*. size 3).

318

319 **4. Discussion and conclusion**

320 Climatic warming is expected to lead to elevational shifts in treelines and
321 shrublines (Myers-Smith et al., 2011; Hofgaard et al., 2013), but our results illustrate
322 that juniper shrublines on the central Tibetan plateau have been unchanged for the last
323 50−200 years. On the central Tibetan Plateau, the climate is characterized by
324 elevated radiation levels and evaporation rates and low precipitation values (You et al.,
325 2010), hence limited moisture rather than low temperatures constrain growth of
326 junipers at shrubline (Liang et al., 2012). Climatic warming without concurrent
327 increases in precipitation will increase the evaporative demand and adversely affect
328 shrub growth and shrubline upward expansion. Thus, upslope advancement of the
329 Tibetan shrubline cannot occur under the warmer and drier conditions that have
330 affected the Tibetan Plateau over the last century (Thompson et al., 2006; Zhu et al.,
331 2011).

332 Shrubline dynamics also depend on the establishment of new individuals
333 (Myers-Smith et al., 2011), and our data illustrate that little or no new recruitment has
334 occurred in our study plots since the 1920s. Future warming (IPCC, 2014) could
335 reduce juniper recruitment even further. Static age structures within treeline ecotones
336 indicate tradeoffs between survival and mortality (Camarero and Gutiérrez, 2004;
337 Wang et al., 2006; Liang et al., 2011), and have also illustrated reduced recruitment at
338 treelines since the 1950s, coincident with warmer and drier climates, in northwest

China (Wang et al., 2006).

We suggest that age structures of juniper shrub plots also can provide insight into recruitment conditions on the central Tibetan Plateau. We acknowledge that the inferences on shrubline dynamics focused on recruitment and rates of advance would be more robust if complemented with growth and mortality data because mortality of shrubs can bias recruitment estimates through time. However, dead shrubs were not found within our shrub plots, making it impossible to estimate mortality rates. Further studies on shrub death and decomposition of dead woody material would help to provide estimates of juniper mortality. Since published growth data revealed the dominant role of moisture availability in juniper wood formation (Liang et al., 2012), the growth data in this study do not promote a deeper understanding of shrubline dynamics in this region.

The slow pace of juniper shrubline change is different from the rapid and extensive shrub expansion observed in Arctic sites where radial growth of shrubs is constrained primarily by low temperatures (Myers-Smith et al., 2011; Naito and Cairns, 2011). However, slow expansion of shrubs also has been reported in the relatively xeric environments of central and eastern Siberia, the interior Alaskan tundra, and continental Mediterranean mountains that receive only seasonal moisture (Wahren et al., 2005; García-Cervigón et al., 2012; Frost and Epstein, 2014). It seems reasonable to suggest, therefore, that warming can exert either negative or positive influences on shrub growth and expansion depending on simultaneous moisture availability (Wahren et al., 2005).

In central Tibet, we hypothesize that recent warming has negatively influenced shrubline dynamics by worsening drought stress, because no significant change in precipitation was observed on the central Tibetan Plateau over the past four centuries and severe droughts were frequent from the 1970s through the 1990s (Yao et al., 2012). In fact, if the frequency of drought increases, the juniper shrubline is at increasing risk of down-slope range shifts. Additional climatic changes also could contribute to exacerbate drought stress: warmer winters could lead to a rapid melting of the snowpack and a decrease in the snowpack thickness could induce drought stress in early spring. Finally, other global drivers such as rising atmospheric concentrations of CO_2 could increase drought tolerance or growth by increasing water-use efficiency of plants (Ainsworth and Long, 2005). However, neither the growth trends (Liang et al., 2012) nor the recruitment patterns we report here match with those expectations.

Climate plays an important role in determining the uppermost elevational limits of arboreal and woody vegetation distribution at global, continental, and regional scales (Körner, 2003), but specific dynamics and related patterns are contingent on local scale processes (Callaway et al., 2002; Holtmeier, 2009). Mounting evidence has shown that the magnitude of shrub expansion in cold biomes such as Arctic tundra is highly reliant on microsite facilitation (e.g., small-scale geomorphic settings, disturbance regimes, or positive plant-environment feedbacks; Tape et al., 2006; Hallinger et al., 2010; Myers-Smith et al., 2011; Naito and Cairns, 2011; Frost and Epstein, 2014; Hagedorn et al., 2014). The presence of neighboring conspecifics exerts considerable control on further shrub establishment and encroachment

383 irrespective of the existence of additional constraining abiotic drivers (Stueve et al.,
384 2011). For example, local microclimatic warming resulting from shrub encroachment
385 is similar in magnitude to regional warming observed over the past century (He et al.,
386 2014). Spatial analysis of junipers in our plots revealed highly clustered distributions
387 and aggregation among different size classes at relatively small scales (<10 m),
388 consistent with the patchy patterns of shrub distribution observed in the landscape
389 around Nam Co Lake (Liang et al., 2012). We infer that such aggregated spatial
390 patterns are produced by conspecific facilitation as has been found in some other
391 treelines (Camarero et al., 2000). Clumping patterns also may stabilize shrubline
392 dynamics by retarding the advance of the ecotone and leading to shrubline stasis
393 (Harsch et al., 2009).

394 Positive interactions among woody plants in similar harsh and dry environments
395 result from enhanced establishment and growth and reduced evaporation that buffer
396 the extreme temperature ranges and improve soil fertility (Callaway et al., 2002;
397 Kikvidze et al., 2005). Thus, it is not surprising that conspecific facilitation at local
398 scales dominates in juniper shrublines. Positive interactions related either to structural
399 or to growth-form effects may allow shrub populations to persist for hundreds of years
400 by preserving specific regeneration-niche features, even under extremely adverse
401 environmental conditions (Holtmeier, 2009). Enhanced longevity linked to slow
402 growth rates and aggregated shrub patterns could act as stabilizing factors (Crawford,
403 2008). If juniper shrublands mainly respond to changes in water availability, climatic
404 warming could induce drought stress and lead to increased mortality of formerly

405 fast-growing individuals (Nobis and Schweingruber, 2013). In central Tibet, such
406 positive interactions could alleviate drought stress and create suitable regeneration
407 niches, leading to enhanced recruitment and upslope shrubline shifts when climatic
408 conditions are favorable. The relatively large amount of recruitment observed prior to
409 the 1920s matches this scenario and supports our hypothesis that local-scale
410 facilitation drives shrubline dynamics.
411
412 **Acknowledgements**
413 This work was supported by the National Natural Science Foundation of China
414 (41471158), the National Basic Research Program of China (2012FY111400), Action
415 Plan for West Development of the Chinese Academy of Science (KZCX2-XB3-08-02).
416 J.J.C. acknowledges funding by ARAID. We appreciate the great support from the
417 Nam Co Monitoring and Research Station for Multisphere Interactions, Chinese
418 Academy of Science.

References

Ainsworth, E.A., Long, S.P., 2005. What have we learned from 15 years of free-air CO2 enrichment (FACE)? A meta-analytic review of the responses of photosynthesis, canopy properties and plant production to rising CO2. *New Phytol*. **165**, 351-372.

Armas, C., Pugnaire, F. I., 2005. Plant interactions govern population dynamics in a semi-arid plant community. *J. Ecol.* **93**, 978-989.

Batllori, E., Camarero, J.J., Ninot, J.M., Gutiérrez, E., 2009. Seedling recruitment, survival and facilitation in alpine *Pinus uncinata* tree line ecotones. Implications and potential responses to climate warming. *Glob. Ecol. Biogeogr.* **18**, 460-472.

Bräuning, A., Mantwill, B., 2004. Summer temperature and summer monsoon history on the Tibetan Plateau during the last 400 years recorded by tree rings. *Geophys. Res. Lett.* **31**, L24205.

Callaway, R.M., Brooker, R.W., Choler P., et al., 2002. Positive interactions among alpine plants increases with stress. *Nature* **417**, 844-848.

Camarero, J. J., Gutiérrez, E., 2004. Pace and pattern of recent treeline dynamics: Response of ecotones to climatic variability in the Spanish Pyrenees. *Clim. Chang.* **63**, 181-200.

Camarero, J.J., Gutiérrez, E., Fortin, M.J., 2000. Spatial pattern of subalpine forest-alpine grassland ecotones in the Spanish Central Pyrenees. *For. Ecol. Manage.* **134**, 1-16.

Case, B.S., Duncan, R.P., 2014. A novel framework for disentangling the scale-dependent influences of abiotic factors on alpine treeline position. *Ecography* **37**, 838–851

Chen, J., Yang, Y., 2011. Seed Plants in Nam Co Basin, Tibet. Meteorological Press, Beijing, China.

Choler, P., Michalet, R., Callaway, R.M., 2001. Facilitation and competition on gradients in alpine plant communities. *Ecology* **82**, 3295–3308.

Crawford, R.M.M., 2008. Plants at the Margin: Ecological Limits and Climate

448 Change. Cambridge University Press, London.
449 Daniels, L.D., Veblen, T.T., 2004. Spatiotemporal influences of climate on altitudinal
450 treeline in northern Patagonia. *Ecology* **85**, 1284-1296.
451 Dullinger, S., Mang, T., Dirnböck, T., et al., 2011. Patch configuration affects alpine
452 plant distribution. *Ecography* **34**, 576-587.
453 Fang, K., Gou, X., Chen, F., et al., 2009. Response of regional tree-line forests to
454 climate change: evidence from the northeastern Tibetan Plateau. *Trees Str. Funct.*
455 **23**, 1321–1329.
456 Fortin, M.J., Dale, M.R.T., 2005. Spatial Analysis: A Guide for Ecologists. Cambridge
457 University Press, Cambridge, UK.
458 Frost, G.V., Epstein, H.E., 2014. Tall shrub and tree expansion in Siberian tundra
459 ecotones since the 1960s. *Glob. Chang. Biol.* **20**, 1264-1277.
460 García-Cervigón, A.I., Mendoza, J.M.O., Gozalbo, M.E., Camarero, J.J., 2012.
461 Arboreal and prostrate conifers coexisting in Mediterranean high mountains differ
462 in their climatic responses. *Dendrochronologia* **30**, 279-286.
463 Grau, O., Ninot, J.M., Blanco-Moreno, J.M., et al., 2012. Shrub-tree interactions and
464 environmental changes drive treeline dynamics in the Subarctic. *Oikos* **121**,
465 1680-1690.
466 Hagedorn, F., Shiyatov, S.G., Mazepa, V.S., et al., 2014. Treeline advances along the
467 Urals mountain range – driven by improved winter conditions? *Glob. Chang. Biol.*
468 **20**, 3530-3543.
469 Hallinger, M., Manthey, M., Wilmking, M., 2010. Establishing a missing link: warm
470 summers and winter snow cover promote shrub expansion into alpine tundra in
471 Scandinavia. *New Phytol.* **186**, 890-899.
472 Harsch, M.A., Hulme, P.E., Duncanm R.P., 2009. Are treelines advancing? A global
473 meta-analysis of treeline response to climate warming. *Ecol. Lett.* **12**, 1040-1049.
474 He, Y., D'Odorico, P., De Wekker, S. F. J., 2014. The relative importance of climate
475 change and shrub encroachment on nocturnal warming in the southwestern United
476 States. *Int. J. Climatol.* **35**, 475-480.
477 Hofgaard, A., Tømmervik, H., Rees, G., Hanssen, F., 2013. Latitudinal forest advance

in northernmost Norway since the early 20th century. *J. Biogeogr.* **40**, 938-949.

Holtmeier, F.K., 2009. Mountain Timberlines: Ecology, Patchiness and Dynamics. Springer, Berlin, German.

Huang, Q., Zhang, C., 2011. Shrubland in Tibet. Forestry Press, Beijing, China.

IPCC, 2014. Climate Change 2014: Synthesis Report. In: Core Writing Team, R.K. Pachauri and L.A. Meyer (Eds.), *Contribution of Working Group I, II and III to the Fifth Assessment Report of the Intergovernmental Panel on Climate Change*. IPCC, Geneva, Switzerland.

Kikvidze, A., Puignaire, F.I., Brooker, R.W., et al., 2005. Linking patterns and processes in alpine plant communities: a global study. *Ecology* **86**, 1395-1400.

Kolishchuk, V.G., 1990. Dendroclimatological study of prostrate woody plants. In: Cook, E.R., Kairiukstis, L.A. (Eds.), *Methods of dendrochronology; applications in the environmental science*. Kluwer Academic Publishers, Dordrecht, pp. 51-55.

Körner, C., 2003. Alpine Plant Life: Functional Plant Ecology of High Mountain Ecosystems. Springer, Berlin, Germany.

Kullman, L., 2002. Rapid recent-margin rise of tree and shrub species in the Swedish Scandes. *J. Ecol.* **90**, 68-77.

Liang E., Wang Y., Eckstein D., Luo T., Little change in the fir tree-line position on the southeastern Tibetan Plateau after 200 years of warming. *New Phytol.* **190**, 760-769.

Liang, E., Dawadi, B., Pederson, N., Eckstein, D., 2014. Is the growth of birch at the upper timberline in the Himalayas limited by moisture or by temperature? *Ecology* **95**, 2453-2465.

Liang, E., Lu, X., Ren, P., Li, X., Zhu, L., Eckstein, D., 2012. Annual increment of juniper dwarf shrubs above the tree line on the central Tibetan Plateau: a useful climate proxy. *Ann. Bot.* **109**, 721-728.

Liu, H., Yin, Y., 2013. Response of forest distribution to past climate change: An insight into future predictions. *Chin. Sci. Bull.* **58**, 4426-4436.

Liu, X., Qin, D., Shao, X., Chen, T., Ren, J., 2005. Temperature variations recovered from tree-rings in the middle Qilian Mountain over the last millennium. *Sci. China*

508 *SER. D* **48**, 521–529.
509 Liu, Y., An, Z., Linderholm, H.W., Chen, D., Song, M., Cai, Q., Sun, J., Tian, H., 2009.
510 Annual temperatures during the last 2485 years in the mid-eastern Tibetan Plateau
511 inferred from tree rings. *Sci. China SER. D* **52**, 348–359.
512 Lv, L., Zhang, Q., 2011. Asynchronous recruitment history of *Abies spectabilis* along
513 an altitudinal gradient in the Mt. Everest region. *J. Plant Ecol.* **5**, 147-156.
514 McIntire, E. J., Fajardo, A., 2009. Beyond description: the active and effective way to
515 infer processes from spatial patterns. *Ecology* **90**, 46-56.
516 Myers-Smith, I.H., Forbes, B.C., Wilmking, M., et al., 2011. Shrub expansion in
517 tundra ecosystems: dynamics, impacts and research priorities. *Env. Res. Lett.* **6**,
518 045509.
519 Myers-Smith, I.H., Hallinger, M., Blok, D., et al., 2015. Methods for measuring arctic
520 and alpine shrub growth: A review. *Earth-Sci. Rev.* **140**, 1-13.
521 Naito, A.T., Cairns, D.M., 2011. Patterns and processes of global shrub expansion.
522 *Prog. Phys. Geog.* **35**, 423-442.
523 Nobis, M. P., Schweingruber, F. H., 2013. Adult age of vascular plant species along an
524 elevational land-use and climate gradient. *Ecography* **36**, 1076-1085.
525 Pellizzari, E., Pividori, M., Carrer, M., 2014. Winter precipitation effect in a
526 mid-latitude temperature-limited environment: the case of common juniper at high
527 elevation in the Alps. *Env. Res. Lett.* **9**, 104021.
528 Post, E., Forchhammer, M.C., Syndonia Bret-Harte, M., et al., 2009. Ecological
529 dynamics across the Arctic associated with recent climate warming. *Science* **325**,
530 1355-1358.
531 Stueve, K.M., Isaacs, R.E., Tyrrell, L.E., Densmore, R.V., 2011. Spatial variability of
532 biotic and abiotic tree establishment constraints across a treeline ecotone in the
533 Alaska Range. *Ecology* **92**, 496-506.
534 Sturm, M., Racine, C., Tape, K., 2001. Increasing shrub abundance in the Arctic.
535 *Nature* **411**, 546-547.
536 Tape, K., Sturm, M., Racine, C., 2006. The evidence for shrub expansion in Northern
537 Alaska and the Pan-Arctic. *Glob. Chang. Biol.* **12**, 686-702.

538 Thompson, L.G., Mosley-Thompson, E., Brecher, H., et al., 2006. Abrupt tropical
539 climate change: Past and present. *Proc. Natl. Acad. Sci. U. S. A.* **103**,
540 10536–10543.
541 Wahren, C.H.A., Walker, M.D., Bret-Harte, S., 2005. Vegetation responses in Alaskan
542 arctic tundra after 8 years of a summer warming and winter snow manipulation
543 experiment. *Glob. Chang. Biol.* **11**, 537-552.
544 Wang, T., Zhang, Q., Ma, K., 2006. Treeline dynamics in relation to climatic
545 variability in the central Tianshan Mountains, northwestern China. *Glob. Ecol.*
546 *Biogeogr.* **15**, 406-415.
547 Wang, X., Wiegand, T., Hao, Z., Li, B., Ye, J., Lin, F., 2010. Species associations in an
548 old-growth temperate forest in north-eastern China. *J. Ecol*. **98**, 674-686.
549 Wiegand, T., Moloney, K. A., 2004. Rings, circles and null-models for point pattern
550 analysis in ecology. *Oikos* **104**, 209-229.
551 Wiegand, T., Moloney, K. A. 2014. Handbook of Spatial Point-Pattern Analysis in
552 Ecology. Chapman & Hall/CRC, Boca Raton, FL, USA.
553 Wilmking, M., Hallinger, M., Van Bogaert, R., et al., 2012. Continuously missing
554 outer rings in woody plants at their distributional margins. *Dendrochronologia* **30**,
555 213-222.
556 Wu, Z., 1983. The Flora of Tibet. Science Press, Beijing, China.
557 Yao, T., Duan, K., Xu, B., Wang, N., Gao, X., Yang, X., 2008. Precipitation record
558 since AD 1600 from ice cores on the central Tibetan Plateau. *Clim. Past* **4**,
559 175-180.
560 Yao, T., Thompson, L., Yang, W., et al., 2012. Different glacier status with
561 atmospheric circulations in Tibetan Plateau and surroundings. Nat. *Clim. Chang.* **2**,
562 663–667.
563 Yang, B., Bräuning, A., Liu, J., Davis, M.E., Shao, Y., 2009. Temperature changes on
564 the Tibetan Plateau during the past 600 years inferred from ice cores and tree rings.
565 Glob. *Planet. Chang*. **69**, 71-78.
566 You, Q., Kang, S., Pepin, N., et al., 2010. Climate warming and associated changes in
567 atmospheric circulation in the eastern and central Tibetan Plateau from a

568 homogenized dataset. *Glob. Planet. Chang*. **72**, 11-24.
569 Zhang, Y., Kang, S., You, Q., Xu, Y., 2011. Climate in the Nam Co Basin. In: Kang S.,
570 Yang, Y., Zhu, L., Yao, T. (Eds.), *Modern environment processes and changes in*
571 *the Nam Co Basin, Tibetan Plateau*. Meteorological Press, Beijing, China, pp.
572 15-25.
573 Zhu, L., Xie, M., Wu, Y., 2010. Quantitative analysis of lake area variations and the
574 influence factors from 1971 to 2004 in the Nam Co basin of the Tibetan Plateau.
575 *Chin. Sci. Bull*. **55**, 1294-1303.
576 Zhu, H., Shao, X., Yin, Z., Xu, P., Tian, H., 2011. August temperature variability in
577 the southeastern Tibetan Plateau since AD 1385 inferred from tree rings.
578 *Palaeogeogr. Palaeoecol. Palaeoecol.* **305**, 84-92.

579 **Figure legends**

580 **Figure 1.** Locations of sampling plots (SW1, SE1, and SE2 plots) and the automatic
581 weather station (AWS) around the Nam Co Lake in the central Tibetan Plateau (a).
582 The upper left inset shows the spatial location of the study area on the Tibetan Plateau.
583 Landscape view of the alpine shrubline (plot SW1) located at an elevation of 4795 m
584 a.s.l. (photograph taken by Y.F. Wang) (b).

585

586 **Figure 2.** Monthly mean air temperature, monthly total precipitation, and monthly
587 evaporation from 1957 to 2013 in Baingoin (4700 m a.s.l.), about 100 km north-west
588 of the Nam Co Lake.

589

590 **Figure 3.** The linear relationship found between age of *Juniperus pingii* var. *wilsonii*
591 shrubs and stem diameter measured at the root collar (a). These data correspond to
592 individuals sampled in plot SE2 (a). The right part in the first row (b) shows the age
593 distribution of shrubs in 50-year classes for the three study plots. The second and third
594 rows (c, d, e) show scatter plots between height and age of shrub individuals in the
595 three study plots (SE1, SW1, and SE2).

596

597 **Figure 4.** Distributions of stem diameters (2.5 cm size-class) at the root collar of
598 sampled *Juniperus pingii* var. *wilsonii* shrubs in the three study plots (SE1, SW1, and
599 SE2).

600

Figure 5. Decadal dynamics of *Juniperus pingii* var. *wilsonii* establishment estimated for three shrublines (SE1, white bars; SW1, gray bars; SE2, dark bars) and reconstructed summer temperature variability presented as *Z*-scores (see more details in Thompson *et al*., 2006). Positive and negative *Z*-scores correspond to warm and cool summer conditions, respectively.

Figure 6. Spatio-temporal dynamics of the *Juniperus pingii* var. *wilsonii* shrubline in plots SE1 (a), SW1 (b), and SE2 (c). Each solid symbol corresponds to an individual shrub that germinated during the period shown at the top and open symbols indicate individuals established during the previous period. Different symbols represent different establishment periods. Note that smaller symbols are used in the last two periods, otherwise they are not visible.

Figure 7. Spatial point patterns and related univariate and bivariate point-pattern analyses of shrubs located in the three study plots (SE1, SW1 and SE2). Three size classes of *Juniperus pingii* var. *wilsonii* individuals (size-class 1, stem diameter at the root collar ≤ 3 cm; size-class 2, stem diameter ≤ 8 cm; size-class 3, stem diameter > 8 cm) were used in the analysis. Figures in the first row show the spatial positions of the three shrub size classes (note that the plot axes are not drawn at the same scale), whereas figures in the second and third rows show the univariate ($O_{11}(r)$ statistic) and bivariate ($O_{12}(r)$ statistic) point-pattern analyses, respectively. Lines with symbols

represent the $O_{11}(r)$ or $O_{12}(r)$ statistics, whereas thin lines correspond to the upper and lower 99% bounds of the simulation envelopes.

Figures

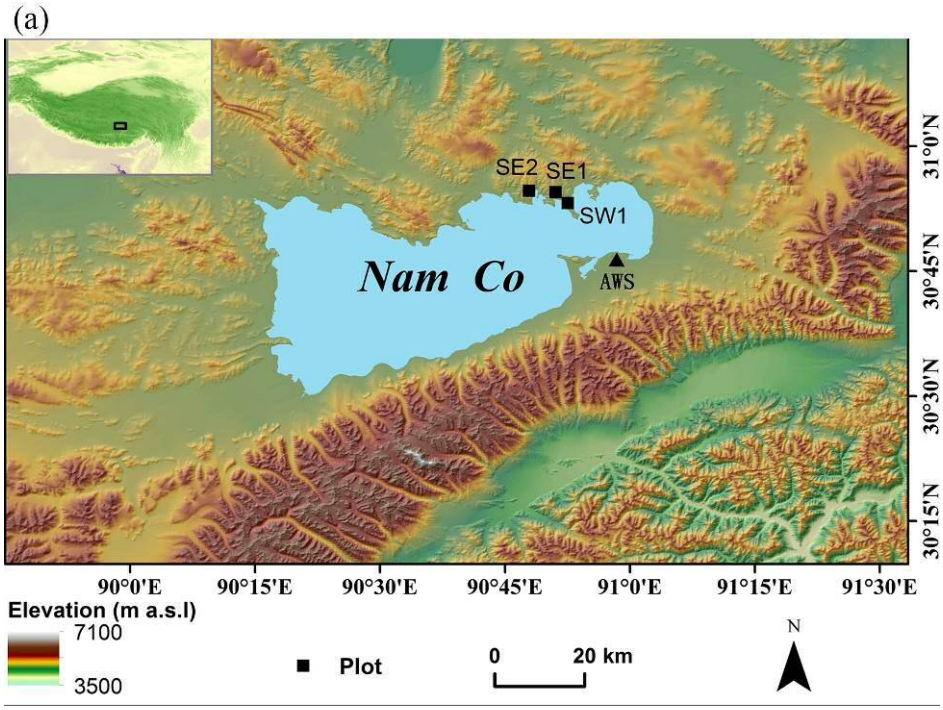

Figure 1

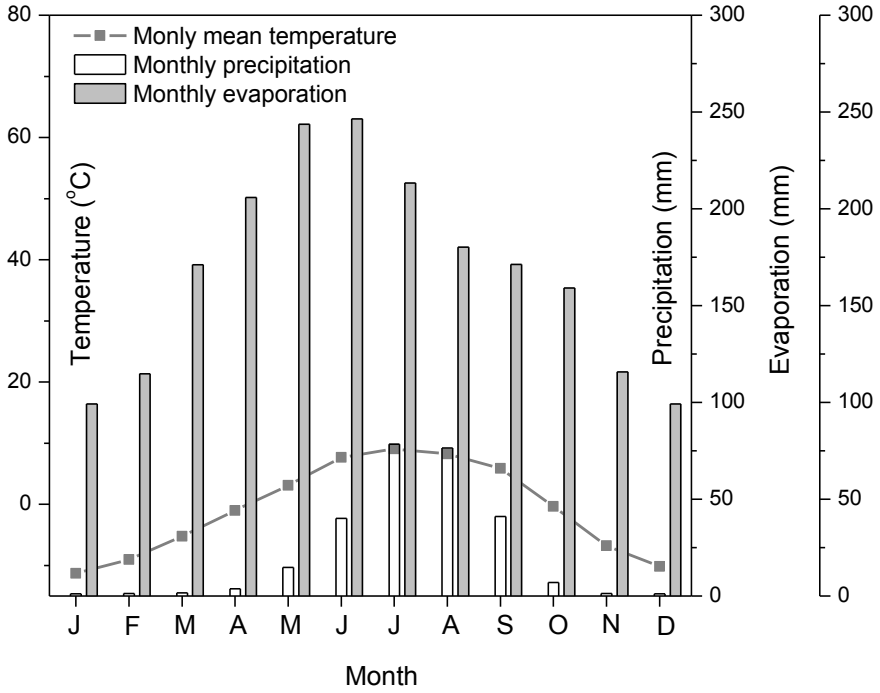
Monly mean temperature
Monthly precipitation
Monthly evaporation
Temperature (°C)
Precipitation (mm)
Evaporation (mm)
Month
J
F
M
A
M
J
J
A
S
O
N
D
80
60
40
20
0
300
250
200
150
100
50
0

Figure 2

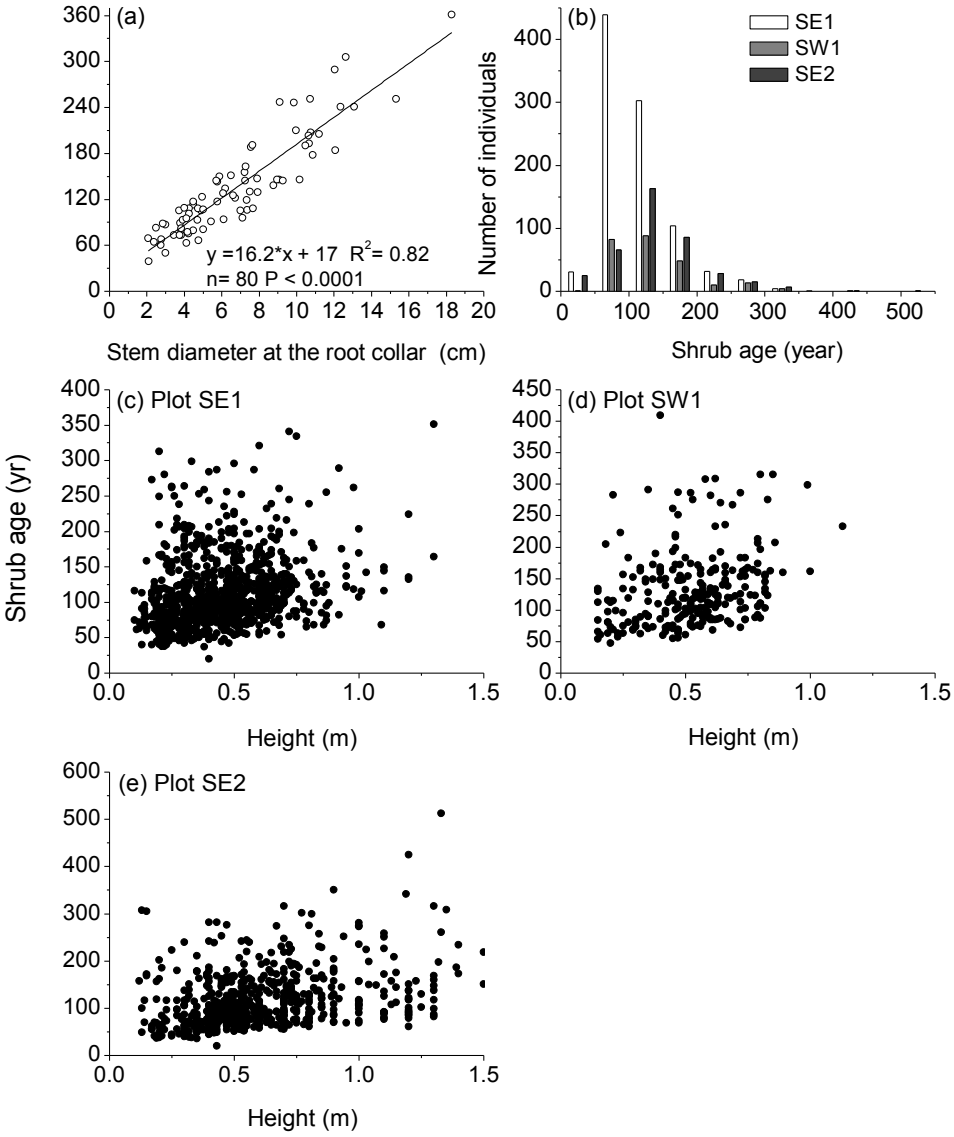

644

645

646 **Figure 3**

647

648

649

650

651

652

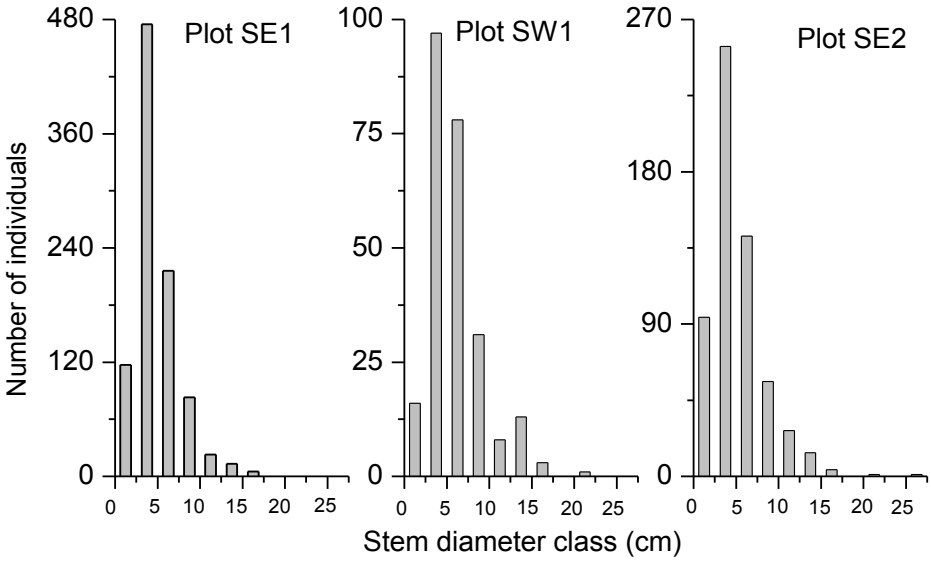
Plot SE1
Plot SW1
Plot SE2
Number of individuals
Stem diameter class (cm)
480
360
240
120
0
100
75
50
25
270
180
90
0 5 10 15 20 25

Figure 4

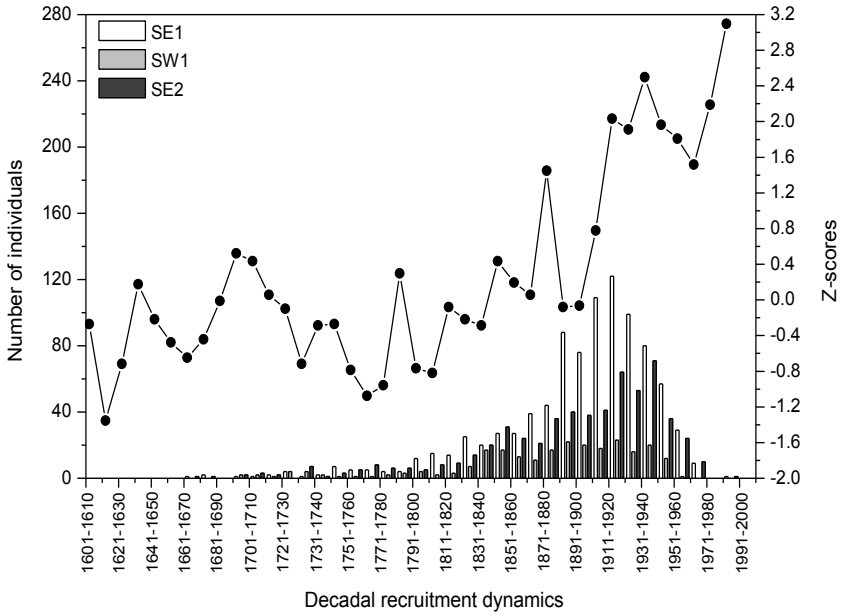

669

670

671 **Figure 5**

672

673

674

675

676

677

678

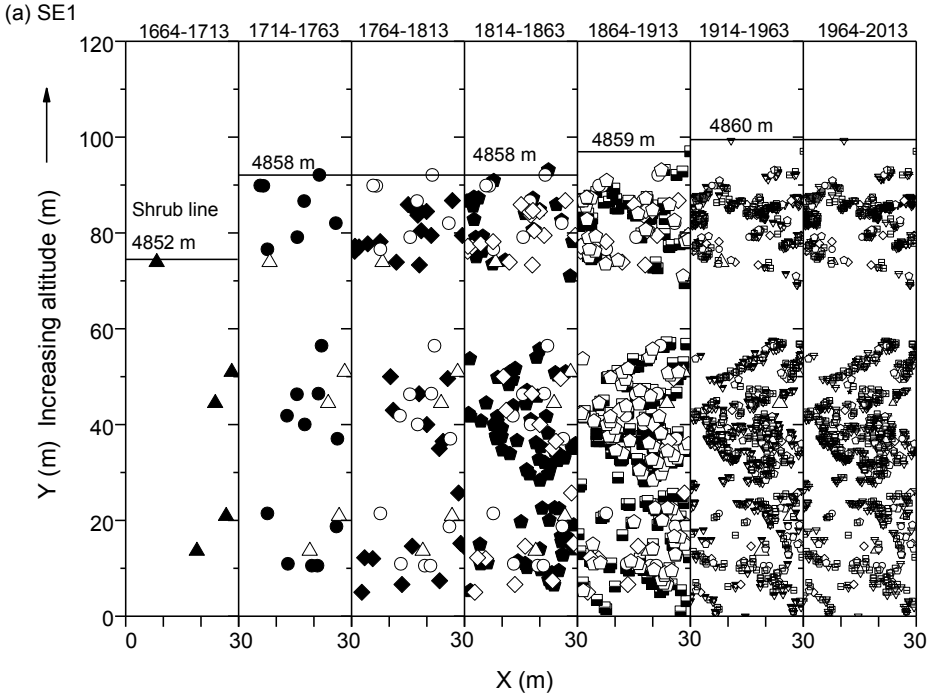
(a) SE1
1664-1713
1714-1763
1764-1813
1814-1863
1864-1913
1914-1963
1964-2013
Shrub line
4852 m
4858 m
4858 m
4859 m
4860 m
Y (m) Increasing altitude (m)
X (m)

679

680

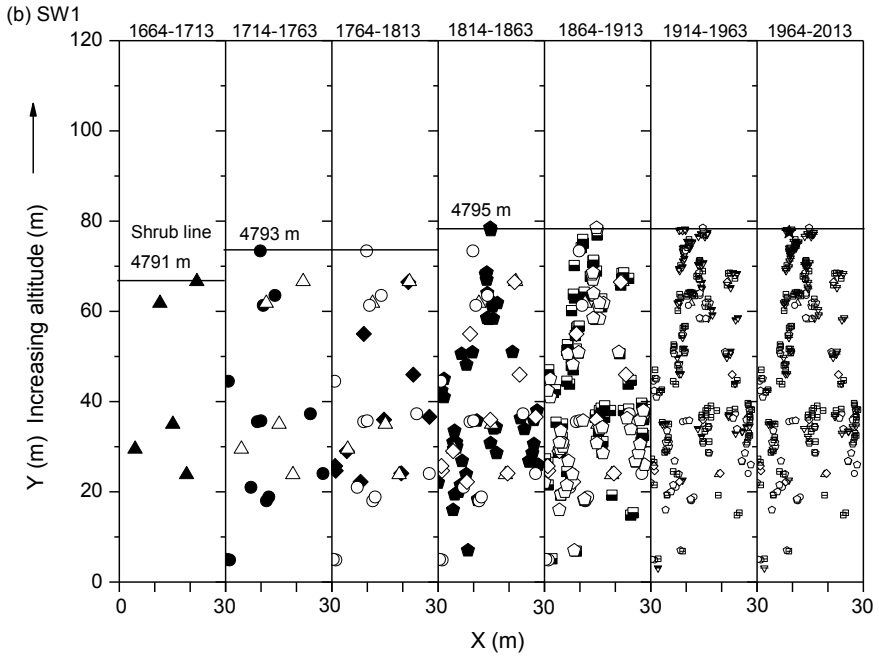
(b) SW1
1664-1713
1714-1763
1764-1813
1814-1863
1864-1913
1914-1963
1964-2013
Shrub line
4791 m
4793 m
4795 m
Y (m) Increasing altitude (m)
X (m)

681

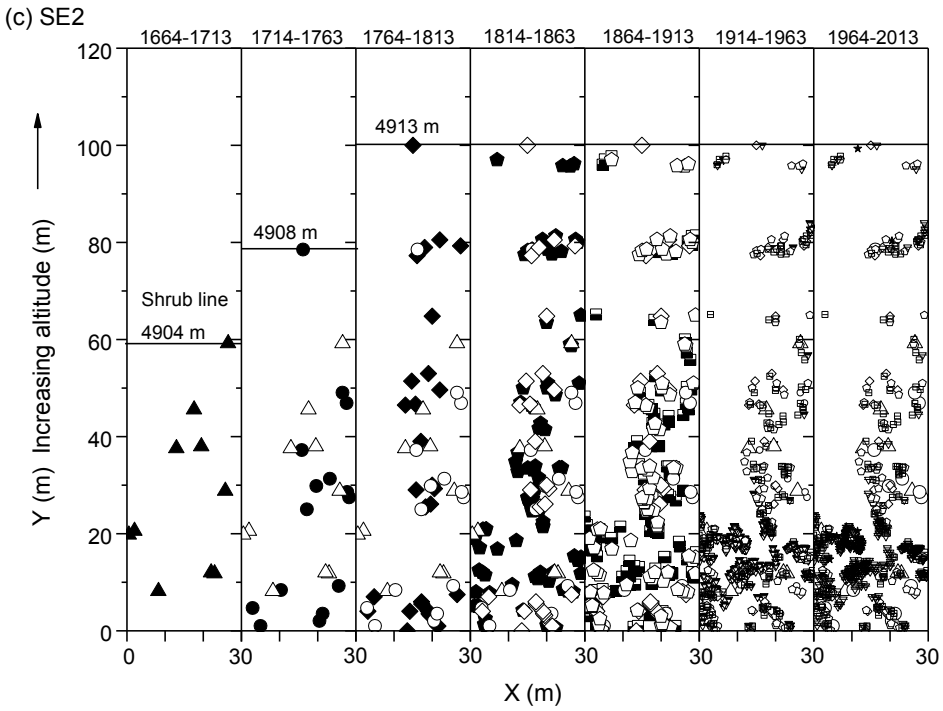

682

683

684

685 **Figure 6**

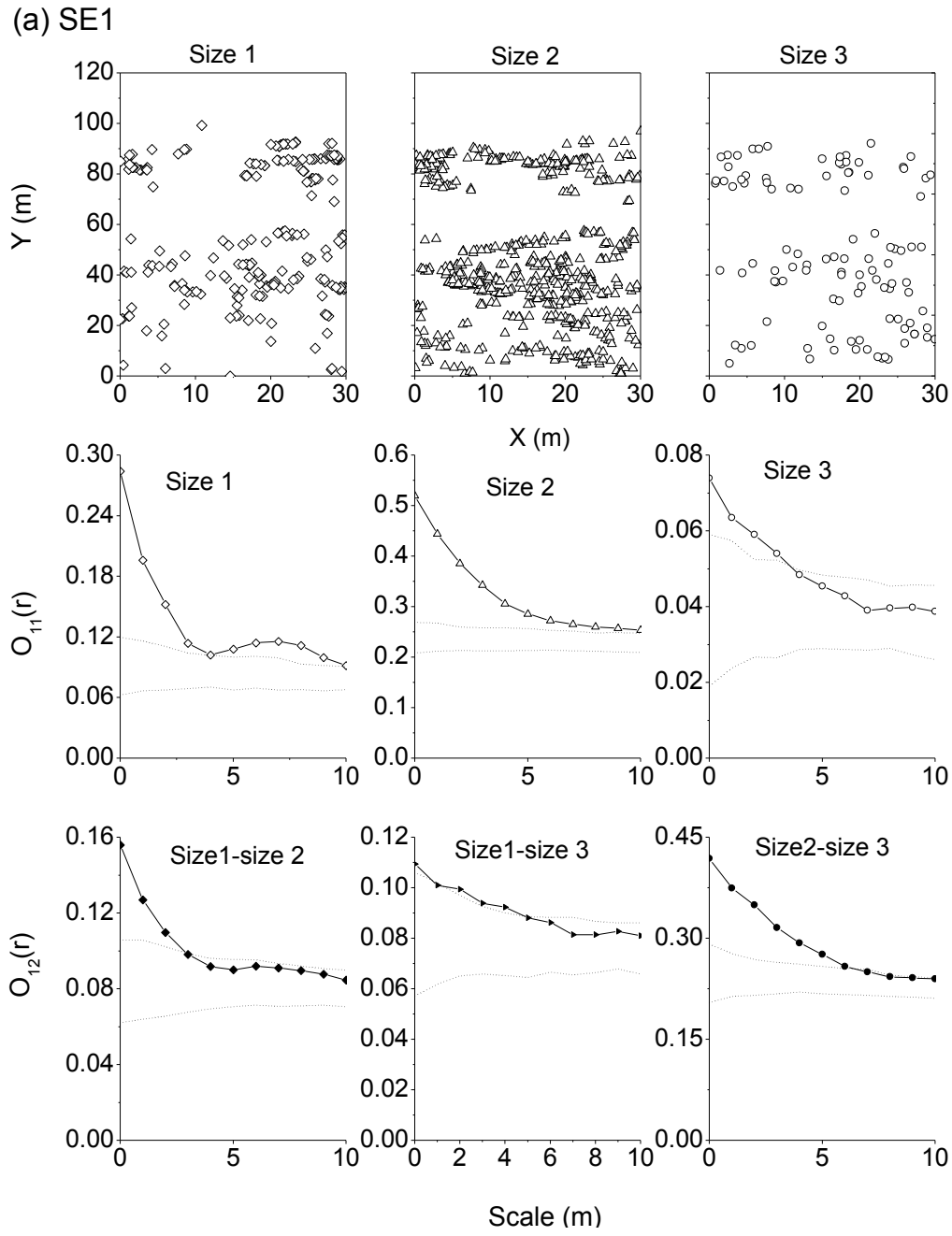
(a) SE1
Size 1
Size 2
Size 3
Y (m)
X (m)
$O_{11}(r)$
$O_{12}(r)$
Size1-size 2
Size1-size 3
Size2-size 3
Scale (m)

686

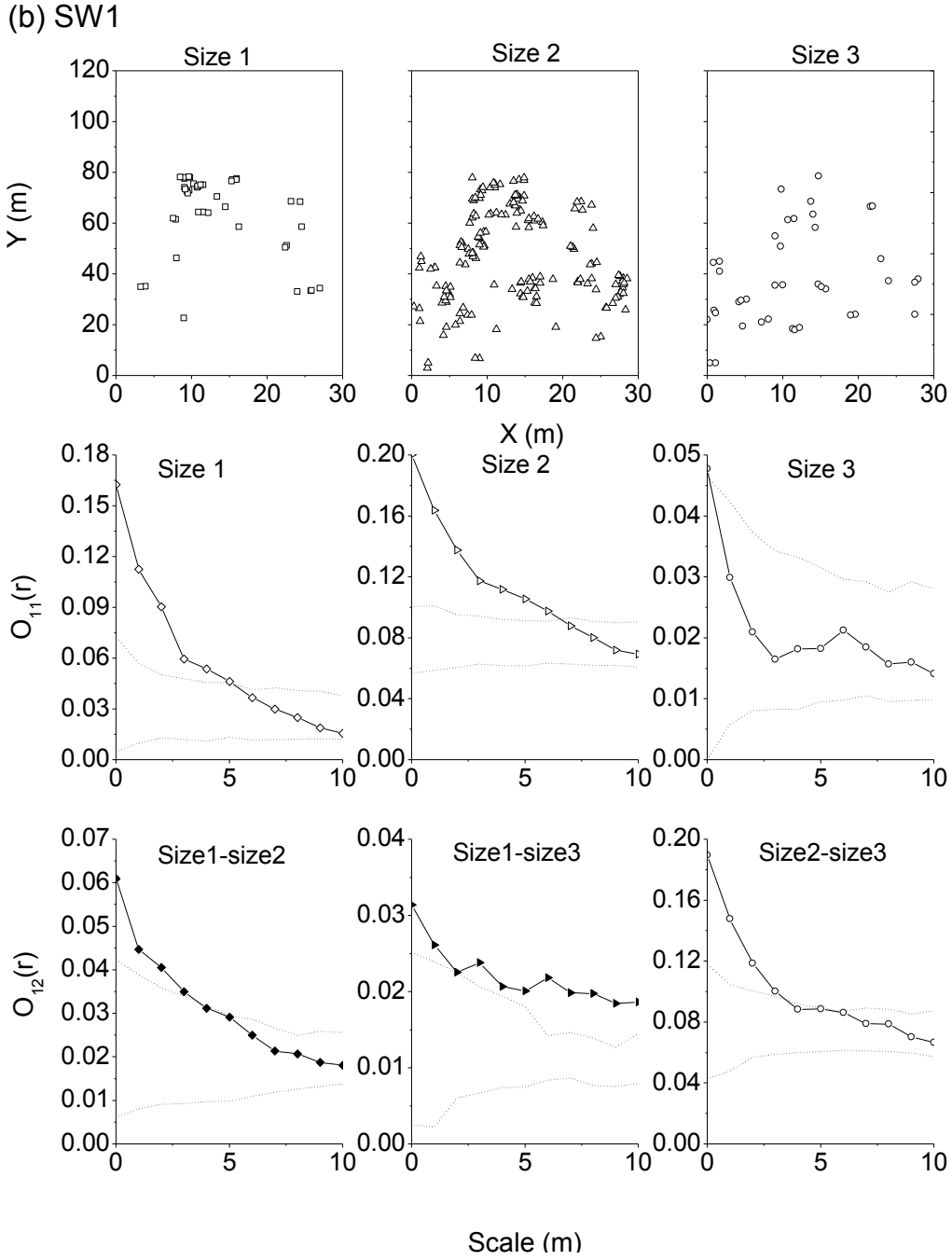
(b) SW1
Size 1
Size 2
Size 3
Y (m)
X (m)
$O_{11}(r)$
$O_{12}(r)$
Size1-size2
Size1-size3
Size2-size3
Scale (m)

687

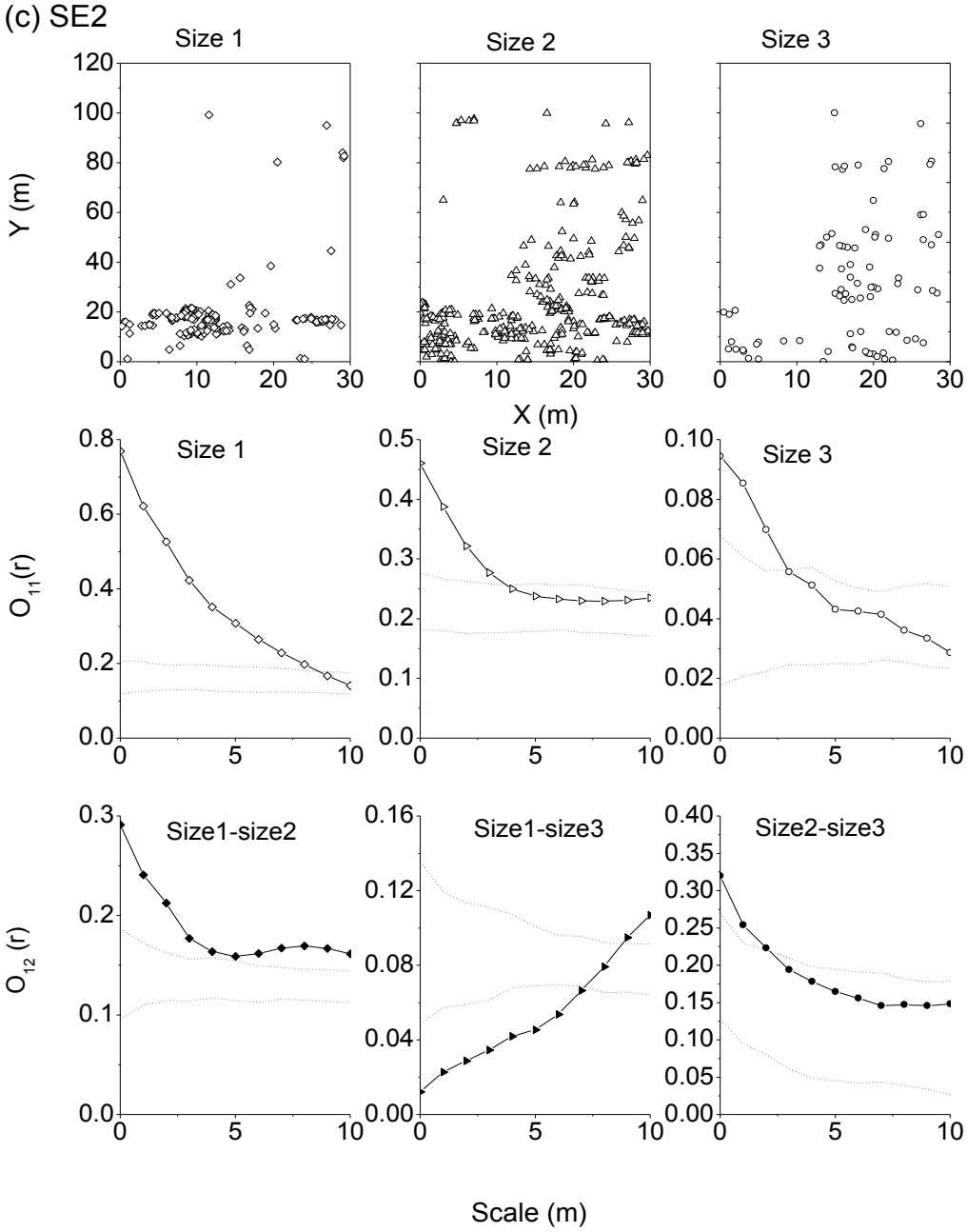

688

689 **Figure 7**

690